Non-analyticity in scale in the planar limit of QCD.

Herbert Neuberger

Rutgers University

on work done in collaboration with **R. Lohmayer**; *Phys. Rev. Lett.*, to appear.

Data updated to December 11, 2011.

Presented at "Numerical Methods for Strongly Coupled Quantum Field Theory and Quantum Gravity"

KITP, U. C. Santa Barbara, CA, 1.30.12

- Original idea: Combining perturbation theory (PT), effective string theory (EST) with a characterization of the crossover between the regimes of validity of PT and EST, it might be possible to get the number σ_N/Λ_N^2 for $N \gg 1$ to reasonable accuracy by analytical means.
- Something like this was tried in the early days of lattice gauge theory, but the corssover was and remains poorly understood. The new simplifying restriction is $N \gg 1$, which makes EST more plausible. In itself, EST makes continuum universal predictions, which is better than what the strong coupling expansion of lattice gauge theory can produce. The original guess was that at $N \gg 1$ the crossover would in itself also have universal aspects.
- I shall start with a simple lattice result and then let it take us to a new qualitative nonperturbative fact about the crossover in 4D pure YM $SU(N)$ gauge theory at $N \gg 1$.

Single eigenvalue density

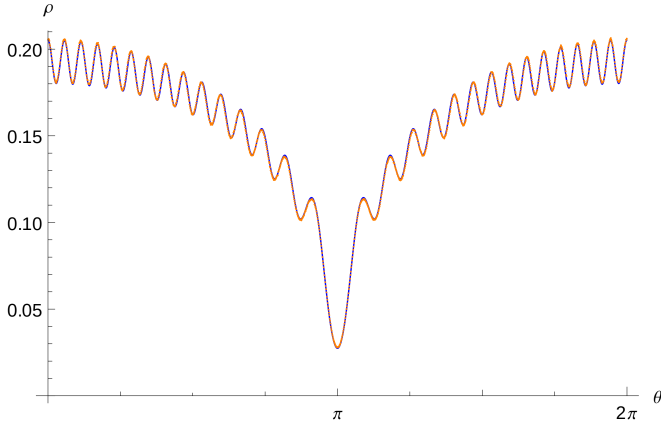

- orange: single eigenvalue density of a square Wilson loop of side ~ 0.5 fermi, in $SU(29)$ pure gauge theory obtained numerically.
- blue: single eigenvalue density given by the heat-kernel eigenvalue density, $\rho_{N=29}^{\mathrm{HK}}(\theta, \tau = 4.015)$ (a known function dependent on a single parameter).

Definition of continuum observables

- Wilson loop matrix associated with a closed spacetime curve $\mathscr{C}$:

$$W_r(\mathscr{C},x,s) = \mathscr{P}\exp\left(i\oint_{x;\mathscr{C}}^{x} A_\mu^r(y,s)dy_\mu\right) \in \mathrm{SU}(N)$$

  r denotes a $SU(N)$ representation and x is a point on $\mathscr{C}$

- $s > 0$ denotes a "smearing parameter" of dimension length squared; smearing is required to make all $W_r(\mathscr{C},x,s)$ finite $SU(N)$ matrices with operator valued entries

- The blue line on the previous plot shows

$$\rho_N(\theta;\mathscr{C},s) = \frac{1}{2\pi N}\sum_{i=1}^{N}\langle\delta(\theta-\theta_i(\mathscr{C},s))\rangle$$

  The $\theta_i(\mathscr{C},s)$ are angles locating the eigenvalues of $W_f(\mathscr{C},x,s)$ on the unit circle; they do not depend on the choice of x and on rigid translations or rotations of $\mathscr{C}$. The CP violating θ_{CP} parameter is set to 0; hence ρ_N is invariant under $\theta \to 2\pi - \theta$.

- Smearing is defined on the next slide

Smearing

- The gauge fields are five dimensional living on $R^4 \times R_+$, the smearing parameter s lives on the R_+
- The usual quantum fields are denoted by $B^f_\mu(x)$ and the $A^f_\mu(x,s)$ are defined for $s \geq 0$ by

$$F_{\mu s} = D_\nu F_{\mu\nu} \qquad\qquad A^f_\mu(x, s=0) = B^f_\mu(x)$$

- The 5D gauge freedom is reduced to a 4D one by $A^f_s(x,s) = 0$
- At $s > 0$ all divergences coming from coinciding spacetime points in products of renormalized elementary fields are eliminated by a limitation on the resolution of the observer, parametrized by s
- Renormalization of the boundary, quantum, fields $B^f_\mu(x)$ proceeds as usual
- The definition of smearing easily extends to any finite UV cutoff including the lattice: replace $D_\nu F_{\mu\nu}$ by the variation of the UV-cutoff–action. The loop in the figure had $s \sim 0.01$ fermi^2
- Smearing extends formally to loop space, with $\mathscr{C}$ parametrized by σ

$$\frac{\partial Tr \left\langle W_f \right\rangle (\mathscr{C}, s)}{\partial s} = \oint d\sigma \frac{\delta^2 Tr \left\langle W_f \right\rangle (\mathscr{C}, s)}{\delta x^2_\mu(\sigma)} \qquad RHS: \text{Lévy Loop Laplacian}$$

- The HK probability density (w.r.t. Haar measure) for an $SU(N)$ matrix W is

$$\mathscr{P}_N^{\text{HK}}(W,t) = \sum_{\text{all } r} d_r \chi_r(W) e^{-\frac{t}{N}C_2(r)}, \qquad \langle \chi_r(W) \rangle = d_r e^{-\frac{t}{N}C_2(r)}$$

  t is a "diffusion time" and d_r, $C_2(r)$ are the dimension and the quadratic Casimir invariant of the irreducible representation r; in the plot $t \to \tau = t(1+1/N)$

- the heat kernel represents a multiplicative random walk on the $SU(N)$ group manifold emanating from the identity

- The HK single eigenvalue distribution is given by

$$\rho^{\text{HK}}{}_N(\theta,t) = \frac{1}{2\pi}\left(1 + \frac{2}{N}\sum_{p=0}^{N-1}(-1)^p \sum_{q=0}^{\infty} \cos((p+q+1)\theta) d(p,q) e^{-\frac{t}{N}C(p,q)}\right)$$

$$C(p,q) = \frac{1}{2}(p+q+1)\left(N - \frac{p+q+1}{N} + q - p\right)$$

$$d(p,q) = \frac{(N+q)!}{p!q!(N-p-1)!}\frac{1}{p+q+1}$$

Casimir dominance

- Looking at the structure of the HK, the goodness of the approximation in the plot can be explained by "Casimir dominance" (at arbitrary fixed N):

$$Tr \langle W_r(\mathscr{C}, x, s)\rangle \approx d_r\; e^{-C_2(r)\mathbf{X}(\mathscr{C},x,s)}$$

- r dependence correct to order g^4 in perturbation theory (small loops)
- r dependence approximately correct for loops dominated by the area law but smaller than ~ 2 fermi (moderately large loops): $\sigma_r \propto C_2(r)$
- r dependence cannot be correct for asymptotically large loops but this talk is restricted to square loops of side $l < 2$ fermi and no screening effects will be seen
- χ_2 goodness of fit estimates rule out exact Casimir dominance for loops in the crossover region 0.3 fermi $< l < 0.7$ fermi
- single eigenvalue distribution depends only on a subset of r's, namely those given by "hook" shaped Young tableaux; so, strictly speaking, " Casimir dominance" could be restricted to only this subset of r's

Structure of single-eigenvalue distribution

- Determined by two main forces: kinematical eigenvalue repulsion and dynamic attraction to unity
- Repulsion produces N peaks at locations consistent with unit determinant
- Attraction to unity squeezes the peaks towards unity
- Depth of valley at minus unity determined by the balance of the two forces
- Adjacent peak-valley swings of order $1/N$
- At infinite N local peaks and valleys merge and ρ becomes monotonic in the 2 segments $(0,\pi),(\pi,2\pi)$; also, a flat global valley centered at π develops for small loops with zero probability eigenvalue density there. For large loops the valley disappears and ρ is non-zero on the entire unit circle
- Thus, at $N=\infty$ a non-analyticity develops in ρ, separating small from large loops
- Durhuus and Olesen (DO) discovered this effect by studying 2D YM gauge theory. In 2D Casimir dominance is exact; so, for the world of eigenvalues they found a phase transition in the limit of large N
- DO found their phase transition by deriving an inviscid Burgers' equation at $N=\infty$ using the 2D YM Makeenko-Migdal loop equations; this PDE determined the single eigenvalue density

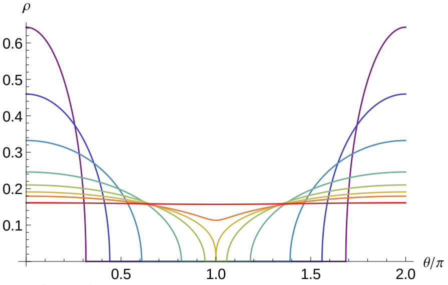

$\tau = 1/4, 1/2, 1, 2, 3, 4, 5, 10$

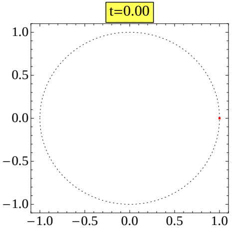

Many of the detailed features of the single eigenvalue distribution at finite N are washed out; one can easily imagine how slowly the finite N eigenvalue distributions evolve with increasing N to their limiting form

From approximate Casimir dominance to something exact

- With Narayanan we conjectured 5 years ago that in d=3,4 DO transitions occur and obey a certain large N universality
- A test in 3D was supportive, but in 4D only indirect arguments could be given
- 4D testing had to wait for a major hardware upgrade of my cluster – an unreasonably onerous task at Rutgers. Later, my talk will focus on first results obtained on the upgraded hardware
- Blaizot and Nowak (BN) conjectured that the large N universality could be understood from the full (not inviscid) Burgers' equation and this proved to be correct
- Thus, the success of the simple fit of the single eigenvalue distribution I showed on my first slide is attributed to an extension of the large-N–DO transition to higher dimensions than 2, inclusive of a large–N universality. This is an exact feature of continuum pure $SU(N)$, asymptotically at large N
- The large–N universal part has to do with eigenvalues close to -1; we need a new observable and a direct definition of the parameter τ

The new observable

- The variable playing the role of τ is chosen to be an overall scale of the loop $\mathcal{C}$; for square loops of side l it is l
- In general, a loop has an infinite number of shape parameters, invariant under dilatations, translations and rotations; the location and overall orientation do not enter and the overall scale is singled out for variation
- We also need a new observable, closer related to the spectrum at -1; start from

$$\mathcal{O}_N(y,\mathcal{C}) = \left\langle \det\left(e^{\frac{y}{2}} + e^{-\frac{y}{2}} W_f(\mathcal{C})\right)\right\rangle = \sum_{k=0}^{N} e^{\left(\frac{N}{2}-k\right)y} \left\langle \chi_k^{\text{asym}}(W_f(\mathcal{C}))\right\rangle$$

- At the transition point $l = l_c$, $\log \mathcal{O}_N$ will have a non-analyticity at $y = 0$ when $N = \infty$; so, we consider the expansion

$$\mathcal{O}_N(y,\mathcal{C}) = a_0(\mathcal{C}) + a_1(\mathcal{C})y^2 + a_2(\mathcal{C})y^4 + O\left(y^6\right), \qquad \omega_N(\mathcal{C}) = \frac{a_0 a_2}{a_1^2}.$$

- $\omega_N(\mathcal{C})$ is similar to a Binder cumulant; many nonuniversal factors cancel out; this is our new observable.

Burgers' equation

- More recently it was noted that for the HK, the new observable is determined by a function that obeys the full Burgers' equation exactly, in agreement with the suggestion of BN:

$$\mathcal{O}_N^{\mathrm{HK}}(y,\tau) = e^{-\frac{N\tau}{8}} \sum_{k=0}^{N} \binom{N}{k} e^{(k-\frac{N}{2})y} e^{\frac{\tau}{2N}(k-\frac{N}{2})^2}$$

$$\phi_N^{\mathrm{HK}}(y,\tau) = -\frac{1}{N}\left(\frac{\partial}{\partial y}\log \mathcal{O}_N^{\mathrm{HK}}(y,\tau)\right)$$

$$\text{Burgers' eq :}\quad \partial_\tau \phi_N^{\mathrm{HK}} + \phi_N^{\mathrm{HK}}\partial_y \phi_N^{\mathrm{HK}} = \frac{1}{2N}\partial_y^2 \phi_N^{\mathrm{HK}}$$

- The initial condition is $\phi_N^{\mathrm{HK}}(y,0) = -\frac{1}{2}\tanh\frac{y}{2}$ and represents the force pushing the eigenvalues toward unity while the PDE itself reflects their spreading as a result of repulsion
- The non-analyticity at $N=\infty$ is a consequence of the compactness of the space the diffusion takes place on; for finite N it is smoothed out by the minimal viscous term present in the PDE.

Non-analytic behavior with Burgers' equation

- At $N = \infty$, Burgers' equation produces a 'shock-wave' singularity at $y = 0$ when τ reaches the critical value $\tau_c = 4$.

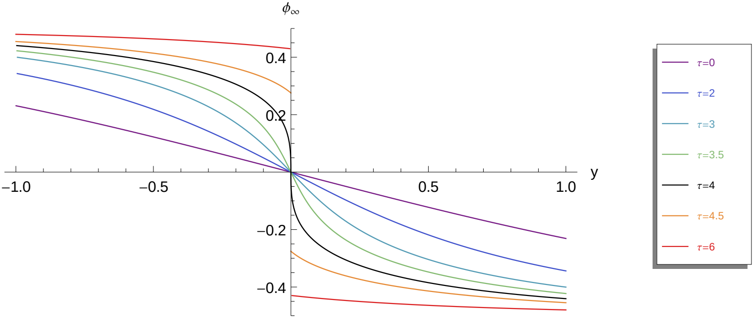

- At finite N the viscous term in Burgers' equation limits the steepness at $y = 0$:

$$\partial_\tau \frac{1}{\partial_y \phi_N^{\text{HK}}|_{y=0}} = 3\omega_N^{\text{HK}}(\tau) - \frac{1}{2}.$$

$\omega^{\text{HK}}{}_N(\tau)$, our observable in the HK case, is designed to capture the $N = \infty$ non-analyticity at $\tau = 4$, as we show on the next slide

About omega

- The inverse slope of ϕ_∞^{HK} at $y = 0$ increases linearly from -4 at $\tau = 0$ to 0 at $\tau = 4$

$$\omega^{\text{HK}}{}_\infty(\tau) = \begin{cases} 1/2, & 0 \le \tau < 4 \\ 1/6, & \tau > 4 \end{cases}$$

resulting in a discontinuous jump in $\phi_\infty(y)$ for $\tau > 4$.

- Singularity is absent at any finite N and develops very slowly as $N \to \infty$

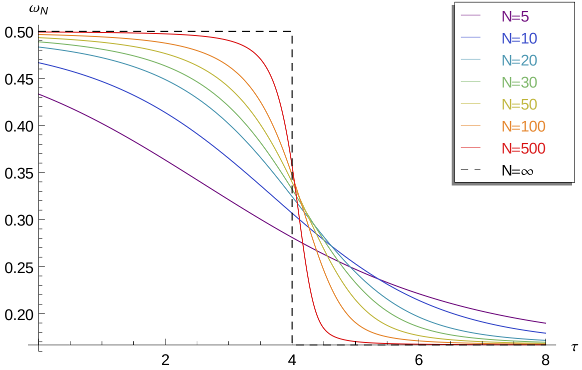

The full relations below come from Burgers' equation in the HK-case, and are expected to hold in 3,4D $SU(N)$ YM too.
From Burgers' equation:

$$\lim_{N\to\infty} N^{-\frac{3}{2}} \left.\frac{a_1}{a_0}\right|_{\tau=4} = \frac{1}{8}\sqrt{\frac{3}{2}\frac{1}{K}}, \qquad K \equiv \frac{1}{4\pi}\Gamma^2\left(\frac{1}{4}\right) \approx 1.046,$$

$$\lim_{N\to\infty} N^{-\frac{3}{2}} \left.\frac{a_2}{a_1}\right|_{\tau=4} = \frac{1}{24}\sqrt{\frac{3}{2}K},$$

$$\lim_{N\to\infty} \omega_N\Big|_{\tau=4} = \frac{1}{3}K^2,$$

$$\lim_{N\to\infty} N^{-\frac{1}{2}} \left.\frac{d\omega_N}{d\tau}\right|_{\tau=4} = -\frac{1}{6}\sqrt{\frac{3}{2}}K(K^2-1).$$

Roots of $\mathscr{O}_N(y,\tau)$ are all on the imaginary axis (an application of the Lee-Yang theorem); in the critical regime (around $y=0$, $\tau=4$) they scale like $N^{-\frac{3}{4}}$.

Setup

- This talk will focus on the non-analyticity and some preliminary data about stringy behavior; we start with the non-analyticity.
- On the lattice we look at square smeared loops smeared with the same action used to generate the gauge configurations (single plaquette Wilson) by an amount S kept in a fixed ratio to the loop lattice area L^2, $S = L^2/110$ ($\partial_S U_\mu = -\left(V_\mu - V_\mu^\dagger - \frac{1}{N}\,\mathrm{Tr}\left(V_\mu - V_\mu^\dagger\right)\right) U_\mu$, with V_μ given by a sum over open $1x1$ loops in directions $\mu, \nu, \nu \neq \mu$; U_μ are lattice link variables, and the V_μ's sum over "staples".
- To extrapolate to the continuum, we compute sequences of square Wilson loops of sides $1 \leq L \leq 9$ for inverse 't Hooft couplings $0.348 \leq b = \frac{1}{g^2 N} \leq 0.374$ at $N = 11, 19, 29$
- Depending on N, we use lattice volumes $8^4, 10^4, 12^4, 14^4, 18^4$ and generate gauge fields by a combination of heat-bath and overrelaxation updates; care is taken to ensure statistical independence of the gauge configurations and to identify the portion of data that has numerically insignificant finite volume dependence
- The coefficients a_0, a_1, a_2 are numerically extracted for each orientation and location of the loop; after averaging one gets one set of $a_{0,1,2}$ for each gauge configuration; subsequent averaging over configurations produces the $a_{0,1,2}$ which determine the estimate for $\omega_N(b, L)$.

Raw data

Numerical results for $N = 19$ (with cubic spline interpolation between measurements):

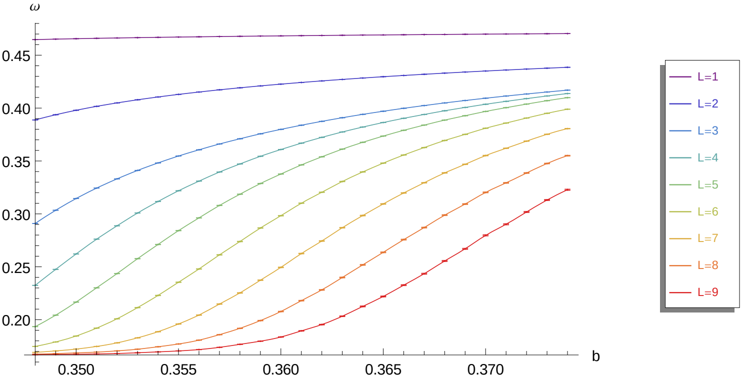

Reminder: $\left\langle \det\left(e^{\frac{y}{2}} + e^{-\frac{y}{2}} W\right)\right\rangle = a_0 + a_1 y^2 + a_2 y^4 + \ldots, \qquad \omega = \frac{a_0 a_2}{a_1^2}.$

Map from ω to τ

- Slow convergence to $N = \infty$ in the HK case indicates that to directly exhibit the $N = \infty$ singularity in 4D prohibitively large N's would be needed
- We adopt a less direct strategy. In continuum language we first define maps for each N from the physical loop size l to $\tau_N(l)$ which are smooth at all N and remain so at $N = \infty$; these maps are shown numerically to converge rapidly as $N \to \infty$, remaining unaffected by the singularity at infinite N in $\omega_N(l)$.
- On the lattice these maps take us from $\omega_N(b, L) \to \tau_N(b, L)$:

$$\omega_N(b, L) = \omega_N^{\text{HK}}(\tau_N(b, L)).$$

- The maps are well defined without any precise assumptions, except an expectation that $approximate$ Casimir dominance holds.
- While formation of the jump in $\omega_N(b, L)$ is slow, we show numerically that $\tau_N(b, L)$ converges rapidly to $\tau_\infty(b, L)$
- Now, $\omega_\infty(b, L) = \omega_\infty^{\text{HK}}(\tau_\infty(b, L)) = \lim_{N\to\infty} \omega_N^{\text{HK}}(\tau_\infty(b, L))$. In 4D continuum we have then $\omega_\infty(l) = \lim_{N\to\infty} \omega_N^{\text{HK}}(\tau_\infty(l))$. $\tau_\infty(l)$ is invertible at $l = l_c$ and C^∞ there. $\omega_N^{\text{HK}}(\tau)$ is known analytically to become singular and this establishes the result also for the 4D case.

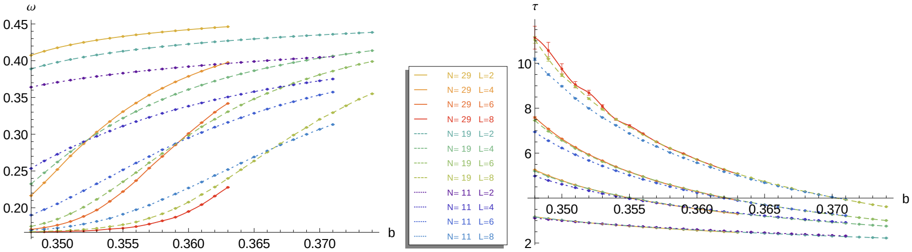

- As N is increased the $\omega_N(b, L)$ curves show a steeper variation
- We see relatively rapid convergence of the map from b to τ at fixed L as N increases
- The physical loop size increases with the lattice loop size and decreases with the lattice coupling b; different intervals of physical size are captured by the different L-labeled curves
- The crossover is identified as the vicinity of $\omega \approx 0.36, \tau \approx 4$ and we have data falling in that range

Continuum limit for τ

- Continuum limit of τ_N is determined by extrapolating $\tau_N(b, L)$ to $L \to \infty$ and $b \to \infty$ correlated by keeping the physical loop size $l = L/L_c(b)$ fixed. This amounts to taking the lattice spacing $a = \frac{l}{L}$ to zero
- $1/L_c(b)$ is the critical deconfinement temperature in lattice units

$$L_c(b) = 0.26 \left(\frac{11}{48\pi^2 b_i(b)} \right)^{\frac{51}{121}} e^{\frac{24\pi^2}{11} b_i(b)}, \qquad b_i(b) = \frac{b}{N} \langle \mathrm{Tr}\, W_{1x1} \rangle \ .$$

- We show one example from the $N = 19$ data below; the deviation from the continuum limit is linear in a^2, as expected

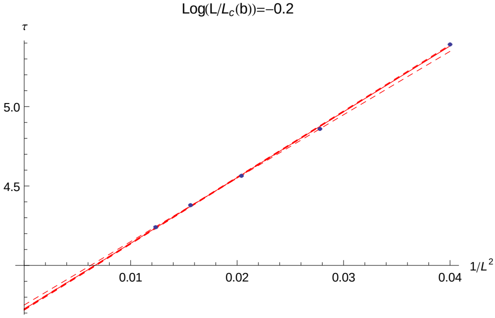

Continuum limit, an example: $\tau_{19}(l)$

$N = 19$:

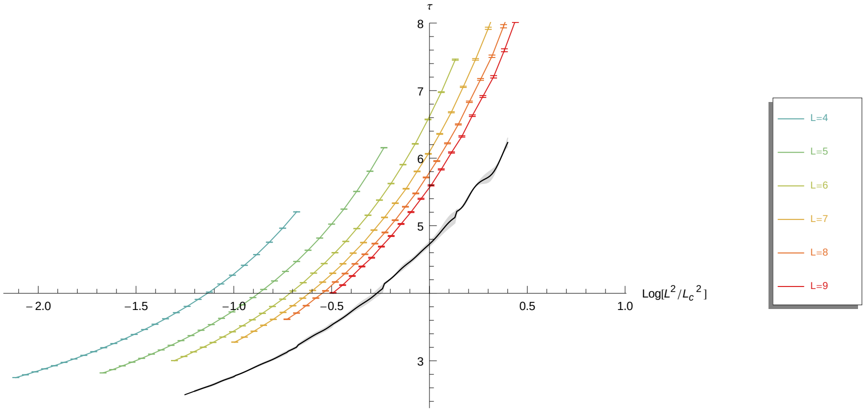

- τ_{19} has a nontrivial continuum limit.
- The $\tau_{19}(l)$ is a smooth function of the physical loop size l.

Continuum limit: $\tau_{19}(l)^{-1}$, $\tau_{11}(l)^{-1}$, $\tau_{29}(l)^{-1}$

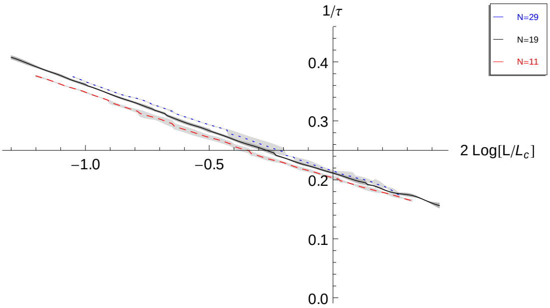

- Weak dependence on N of continuum limit $\tau_N(l)$ for $N = 11, 19, 29$.
- Meaning of universality: in the vicinity of the critical point $\tau = 4$, we can replace $\omega_N(l, s = fixed)$ by $\omega_N^{\mathrm{HK}}(\tau_\infty(l))$ without changing the singular large-N properties.
- Dependence on l is consistent with asymptotic freedom.
- If we extract a tree-level calculable, shape-dependent, factor from τ we obtain a particular effective coupling constant at scale l

Universal exponent $3/2$

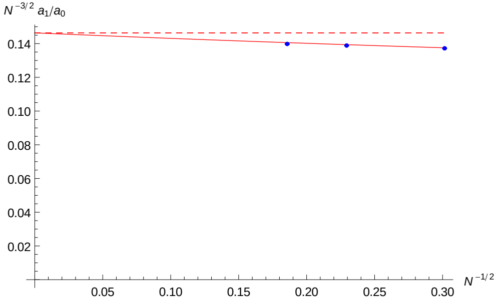

- red, dashed: HK at $N = \infty$
  blue: data for $L = 6$ at $N = 29$, $N = 19$ and $N = 11$
  (the data is extrapolated to $\tau = 4$ using spline interpolation)
  red, solid: HK at finite N, as a function of N, independent of data
- Linear fit of $\log \frac{a_1}{a_0}$ vs $\log N$ leads to exponent of 1.52.
- The way of defining τ from ω makes the ratio $\frac{a_2}{a_1}$ dependent on the one plotted and automatically guarantees the exponent $1/2$ in the τ dependence at criticality.

Universal exponent $3/4$

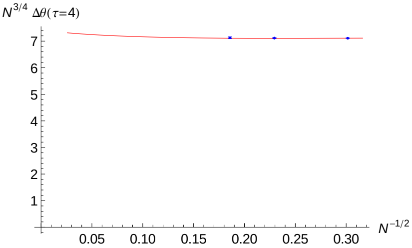

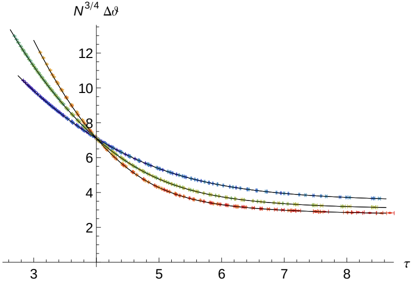

- $\Delta\theta$ is the angular difference between the two peaks in the single eigenvalue density closest to $\theta = \pi$: red solid line is obtained from the the HK
- At fixed τ, $\Delta\theta$ does not depend on L.
- Linear fit of $\log \Delta\theta(\tau = 4)$ vs $\log N$ results in exponent of 0.74 (exponent for heat-kernel model: $3/4$)

Summary and Outlook

- Confirmation that there is a large-N phase transition for smeared Wilson loops in Euclidean 4D continuum $\mathrm{SU}(N)$ gauge theory at a critical loop size.
- Confirmation that the transition has universal properties with universality class defined in terms of the HK with characteristic exponents $3/2$, $3/4$ in the characteristic polynomial and single eigenvalue density respectively
- A gap in the Wilson loop eigenvalue-distribution at $N = \infty$ means – in Hamiltonian language – that 't Hooft disorder loop operators cannot be arbitrarily thin at $N = \infty$.
- Having established a non-analyticity at $N = \infty$ the main question is whether it feeds into the *connected* S-matrix where each matrix element is taken as the first non-vanishing term in the $\frac{1}{N}$ expansion: If it does, this opens up many questions; if it does not, the mechanism shielding the S-matrix needs to be understood. A related question is whether the $\frac{1}{N}$ expansion is equivalent to the scheme of "dual topological unitarization".

Side comments on smearing

It is essential to better understand the observable impact of smearing; some comments

- Field theory: expansions in $s \to 0$ and $s \to \infty$ for a kink-free closed loop

$$\log\left[Tr\left\langle W_r\right\rangle\right](\mathscr{C},s) = g^2_{eff}(\mathscr{C})\left[\mathscr{A}_0(\mathscr{C})\frac{l}{\sqrt{s}} + \mathscr{A}_1(\mathscr{C}) + \mathscr{O}(\frac{\sqrt{s}}{l})\right]$$

$$\log\left[Tr\left\langle W_r\right\rangle\right](\mathscr{C},s) = G^2_{eff}(\mathscr{C})\left[\frac{l^4}{s^2}\mathscr{B}_0(\mathscr{C}) + \frac{l^6}{s^3}\mathscr{B}_1(\mathscr{C}) + \mathscr{O}(\frac{l^8}{s^4})\right]$$

- At fixed l, $s \to \infty$ produces an OPE with well defined "condensates". $s \to 0$ produces a perimeter divergence. For QED, both effective coupling constants become e_0^2 and $\mathscr{A}_1(\mathscr{C})$ becomes Stodolsky's "photon number"; when separated kinks in the loop are allowed, the expansion $s \to 0$ also has a $\log\frac{l}{\sqrt{s}}$ term
- A variant of smearing works in the Hamiltonian framework
- String theory: if the holy grail is found, we shall have a definition of loop space functionals, the loop Laplacian acting on them and a solution to the Makeenko-Migdal equations. Then, smearing is guaranteed to extend to this loop space because it is the solution of the diffusion equation on it.

String Tension I

We now turn to preliminary stringy data.
String Tension from Creutz ratios and fit to full functional form (for 18p4n11b366 at $s = 0.2$); x-axis labels are meaningless.

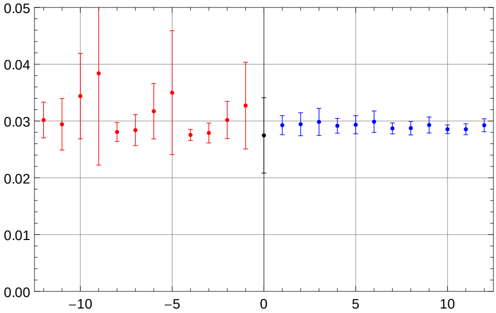

Blue data result from a fit to the effective string asymptotic expansion neglecting terms of order inverse area and higher. Also, a constant and a perimeter term are included. Red data is obtained from Creutz ratios. Traces of $L \times L$ and $L \times (L+1)$ loops were collected. In each colored set results from fits to data in different ranges of L are shown.

String Tension II

Smearing is crucial in making corner and perimeter terms finite, while anything universal coming from the effective string theory should be smearing independent.

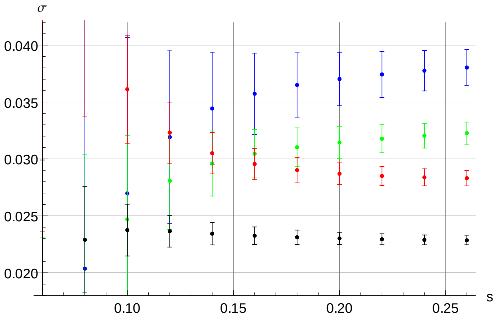

s-dependence of the string tension (for 18p4n11, $b \in \{0.360, 0.363, 0.366, 0.370\}$; fit range $L \in \{6, 10.5\}$)

String Tension III

b-dependence of the string tension (for 18p4n11, $s = 0.26$; fit range $L \in \{6, 10.5\}$) and horizontal lines are at $\sigma L_c^2 = 2.658 \pm 0.018$

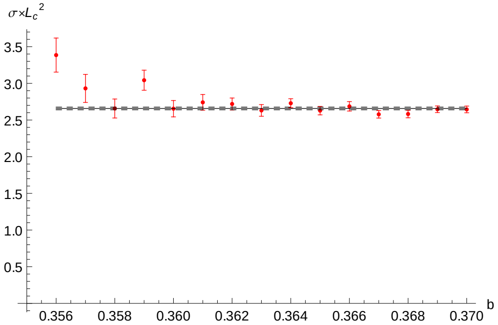

$L_c(b)$ is a length scale defined by the two loop β-function with the coupling b replaced by the tadpole improved coupling. Continuum limit is approached going to the right.

String Tension IV

b-dependence of the string tension (for 18p4n11 and 14p4n19, $s = 0.2$; fit range $L \in \{6, 10.5\}$)
$N = 11$ (red), $N = 19$ (blue), $s = 0.20$
Fits: $N = 11$: 2.640(25) (black line); $N = 19$: 2.603(28) (grey line).

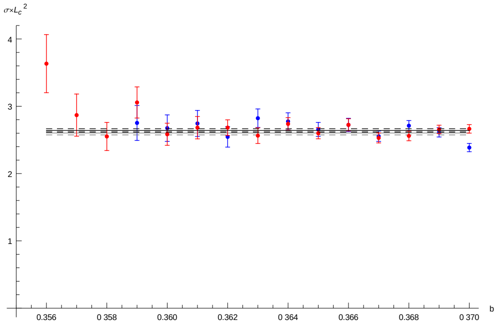

$1/N^2$ correction between $N = 11, 19$ is or order one percent, below statistical uncertainty.